JCI The Journal of Clinical Investigation

17β-Estradiol inhibits Ca^{2+}-dependent homeostasis of airway surface liquid volume in human cystic fibrosis airway epithelia

Ray D. Coakley, … , Steven L. Young, Robert Tarran

J Clin Invest. 2008;118(12):4025-4035. https://doi.org/10.1172/JCI33893.

Research Article

Normal airways homeostatically regulate the volume of airway surface liquid (ASL) through both cAMP- and Ca^{2+}-dependent regulation of ion and water transport. In cystic fibrosis (CF), a genetic defect causes a lack of cAMP-regulated CFTR activity, leading to diminished Cl^- and water secretion from airway epithelial cells and subsequent mucus plugging, which serves as the focus for infections. Females with CF exhibit reduced survival compared with males with CF, although the mechanisms underlying this sex-related disadvantage are unknown. Despite the lack of CFTR, CF airways retain a limited capability to regulate ASL volume, as breathing-induced ATP release activates salvage purinergic pathways that raise intracellular Ca^{2+} concentration to stimulate an alternate pathway to Cl^- secretion. We hypothesized that estrogen might affect this pathway by reducing the ability of airway epithelia to respond appropriately to nucleotides. We found that uridine triphosphate–mediated (UTP-mediated) Cl^- secretion was reduced during the periovulatory estrogen maxima in both women with CF and normal, healthy women. Estrogen also inhibited Ca^{2+} signaling and ASL volume homeostasis in non-CF and CF airway epithelia by attenuating Ca^{2+} influx. This inhibition of Ca^{2+} signaling was prevented and even potentiated by estrogen antagonists such as tamoxifen, suggesting that antiestrogens may be beneficial in the treatment of CF lung disease because they increase Cl^- secretion in the airways.

17β-Estradiol inhibits Ca^{2+}-dependent homeostasis of airway surface liquid volume in human cystic fibrosis airway epithelia

Ray D. Coakley,[1] Hengrui Sun,[1] Lucy A. Clunes,[1] Julia E. Rasmussen,[1] James R. Stackhouse,[1] Seiko F. Okada,[1] Ingrid Fricks,[2] Steven L. Young,[3] and Robert Tarran[1]

[1]Cystic Fibrosis/Pulmonary Research and Treatment Center, [2]Department of Pharmacology, and [3]Division of Reproductive Endocrinology and Infertility, University of North Carolina, Chapel Hill, North Carolina, USA.

Normal airways homeostatically regulate the volume of airway surface liquid (ASL) through both cAMP- and Ca^{2+}-dependent regulation of ion and water transport. In cystic fibrosis (CF), a genetic defect causes a lack of cAMP-regulated CFTR activity, leading to diminished Cl^- and water secretion from airway epithelial cells and subsequent mucus plugging, which serves as the focus for infections. Females with CF exhibit reduced survival compared with males with CF, although the mechanisms underlying this sex-related disadvantage are unknown. Despite the lack of CFTR, CF airways retain a limited capability to regulate ASL volume, as breathing-induced ATP release activates salvage purinergic pathways that raise intracellular Ca^{2+} concentration to stimulate an alternate pathway to Cl^- secretion. We hypothesized that estrogen might affect this pathway by reducing the ability of airway epithelia to respond appropriately to nucleotides. We found that uridine triphosphate–mediated (UTP-mediated) Cl^- secretion was reduced during the periovulatory estrogen maxima in both women with CF and normal, healthy women. Estrogen also inhibited Ca^{2+} signaling and ASL volume homeostasis in non-CF and CF airway epithelia by attenuating Ca^{2+} influx. This inhibition of Ca^{2+} signaling was prevented and even potentiated by estrogen antagonists such as tamoxifen, suggesting that antiestrogens may be beneficial in the treatment of CF lung disease because they increase Cl^- secretion in the airways.

Introduction

Mucus clearance is an important aspect of innate defense in the mammalian lung (1). The rate of mucus clearance is set by the volume of airway surface liquid (ASL) on airway surfaces (2). The ASL is composed of a periciliary liquid layer (PCL) that lubricates the cell surface and a mucus layer that traps airborne particles and pathogens (3). Adenosine (ADO) and ATP act as physiological ligands that stimulate P1 and P2 subtypes of purinergic receptors to raise cAMP and Ca^{2+} levels, respectively, so that Cl^- secretion is activated (4–6). Normal airways can secrete sufficient Cl^- to hydrate the mucus layer by raising either cAMP levels to stimulate CFTR or Ca^{2+} to stimulate an alternate Cl^- channel (7). Cystic fibrosis (CF) airways lack CFTR but under appropriate conditions can still secrete Cl^- in response to extracellular nucleotides.

CF lung disease is typified by mucus plugging, which reflects a failure of CF airway epithelia to adequately hydrate mucus on their surfaces, particularly in response to infectious challenges (8, 9). We have proposed that CF airways are more vulnerable to adverse events such as viral infections, since they lack the "reserve capacity" to secrete additional ASL beyond normal day-to-day events due to the absence of functional CFTR. For example, respiratory syncytial virus infections upregulate ecto-ATPases that degrade ASL ATP (2). This has moderate effects on non-CF ASL volume homeostasis, since these airways can still secrete Cl^- via CFTR. However, CF ASL volume homeostasis is markedly reduced and ASL volume is depleted to levels incompatible with mucus clearance due to the lack of extracellular ATP to raise Ca^{2+}_i levels and initiate Cl^- secretion (2). Thus, having only 1 pathway for Cl^- secretion leaves CF airways more vulnerable to acute exacerbations due to reduced mucus hydration and decreased mucus clearance, which pave the way for chronic bacterial infection of the lung.

Sexual phenotype is now recognized as being a risk factor for chronic lung disease. For example, approximately 70% of early onset chronic obstructive pulmonary disease patients are female (10), and adult females also suffer more severely from asthma and some lung carcinomas (11). The incidence of CF is not sex linked (12). However, previous studies have indicated that females with CF (a) exhibit more rapid rates of decline in lung function; (b) acquire *Pseudomonas aeruginosa* earlier (13); (c) have increased frequency of acute exacerbation (14); (d) have decreased life spans as compared with males with CF (15); and (e) develop more diffuse lung disease (16). While the results of such studies are not uniform, the largest population study to date suggests a sex-related disadvantage persists (15).

In premenopausal women, the major circulating estrogen is 17β-estradiol (E2), which is produced by the ovaries. During menses, circulating E2 falls to approximately 0.1 nM and then increases through the follicular phase, achieving a peak concentration of approximately 3 nM during the few days prior to ovulation. Estrogen receptors (ERs) are also expressed in males and stimulated by E2 that is formed as a breakdown product of testosterone (17). However, serum E2 levels are much lower (< 0.1 nM) and do not fluctuate. ERs are traditionally thought to act at the transcriptional level, where they translocate from the cytoplasm into the nucleus

Nonstandard abbreviations used: ADO, adenosine; ASL, airway surface liquid; BHK, baby hamster kidney; CF, cystic fibrosis; E2, 17β-estradiol; ER, estrogen receptor; HBEC, human bronchial epithelial culture; IP, inositol phosphate; I_{sc}, short-circuit current; ISO, isoproterenol; mOr, monomeric orange fluorescent protein; PCL, periciliary liquid layer; PD, potential difference; PFC, perfluorocarbon; $P2Y_2$-R, $P2Y_2$ receptor; qPCR, quantitative PCR; TXN, tamoxifen; UTP, uridine triphosphate.

Conflict of interest: The authors have declared that no conflict of interest exists

Citation for this article: *J. Clin. Invest.* doi:10.1172/JCI33893.

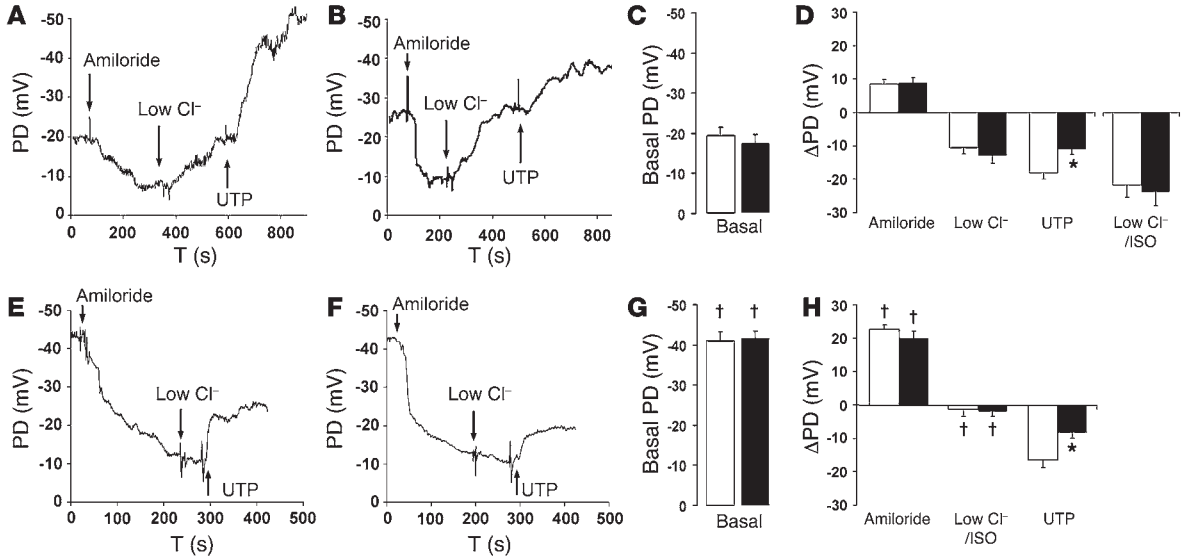

Figure 1

UTP-activated Cl^- secretion changes with the menstrual cycle. Females with and without CF calculated their high– and low–E2 level days based on the onset of menses, and nasal PDs were recorded at these times. White bars represent low–E2 level days and black bars represent high–E2 level days. (**A** and **B**) Typical traces showing sequential addition of amiloride, a low Cl^- solution, and UTP on low and high days respectively. T, time. (**C**) Paired mean basal nasal PDs measured on low– and high–E2 level days (n = 12). (**D**) Paired mean changes in nasal PD in normal subjects on low- and high-level E2 days following amiloride addition and following perfusion of a low Cl^- solution and a low Cl^- solution containing 100 μM UTP added in the continued presence of amiloride to measure the UTP-activated Cl^- secretory response (n = 12). In a separate experiment, perfusion of a low Cl^- solution containing amiloride with 100 μM ISO in a subset of the subjects tested in **A**–**C** (n = 6). (**E** and **F**) Typical traces showing sequential addition of amiloride, a low Cl^- solution with 100 μM ISO, and UTP on low- and high-level E2 days, respectively, in CF subjects. (**G**) Paired mean basal CF nasal PDs measured on low– and high–E2 level days (n = 10). (**H**) Paired mean changes in nasal PD in CF patients following amiloride addition and following perfusion of a low Cl^- solution containing 100 μM ISO and a low Cl^- solution containing 100 μM UTP added in the continued presence of amiloride to measure the UTP-activated Cl^- secretory response (n = 10). $^*P < 0.05$ difference in UTP secretion between low– and high–E2 level days. $^\dagger P < 0.05$ compared with non-CF.

to exert their effects (18). However, rapid nongenomic actions of E2 are now recognized, and many signaling pathways have been identified as targets of rapid E2 action, including Ca^{2+}(19) and inositol triphosphate (IP_3) (20, 21).

We hypothesized that increases in E2 levels in the late follicular phase would reduce the ability of females with CF to regulate second messengers and secrete sufficient Cl^- for efficient ASL volume homeostasis. To test this hypothesis, we measured nasal potential differences (PDs) in normally cycling reproductive-age women at different points during the menstrual cycle. These experiments revealed that a 4-fold increase in E2 was accompanied by a 50% inhibition of UTP-stimulated Cl^- secretion in vivo. To further investigate the mechanism underlying this phenomenon, we utilized polarized airway cultures and ER-null cell lines transiently expressing ERα or ERβ and found that activation of ERα inhibits Ca^{2+} influx that impairs Cl^- secretion and ASL volume homeostasis. Finally, we found that ER antagonists could reverse the effects of E2 and even potentiate the $P2Y_2$ response, suggesting that they may be useful adjuncts in treating lung disease in females with CF.

Results

In vivo measurements of UTP-stimulated Cl^- secretion. We tested the hypothesis that high E2 levels inhibited UTP-stimulated Cl^- secretion in vivo by measuring nasal PDs in female subjects with and without CF who were not taking hormonal contraceptives and who experienced regular menstrual cycles. Paired nasal PDs were recorded during menses, when E2 is lowest, and 12 days after the onset of menses, when E2 levels were higher. Once a maximal stable baseline PD was detected, amiloride was added to inhibit ENaC, followed by amiloride plus a low Cl^- solution to generate the maximal gradient for Cl^- secretion (Figure 1). Changes in E2 levels were measured at the time of PD recording and changed from 0.1 nM during menses to 0.5 nM during the periovulatory phase (both n = 12). The basal and amiloride-sensitive PDs were significantly greater in subjects with CF compared with subjects without CF, and the low Cl^-/isoproterenol (Cl^-/ISO) responses were absent in CF subjects (Figure 1). However, there was no difference in the magnitude of the basal or amiloride-sensitive PDs between the low– and high–E2 level days for either subjects without CF (Figure 1, A–D) or those with CF (Figure 1, E–H). The UTP-stimulated PDs were reduced by approximately 40% on high–E2 level days in subjects without CF and by approximately 50% on high–E2 level days in subjects with CF (Figure 1, D and H) (suggesting that E2 does indeed inhibit UTP-mediated Cl^- secretion in vivo). In contrast with the cycle-dependent changes in the UTP-stimulated PDs, the ISO-stimulated PDs, which were only present in subjects without CF, remained stable during the menstrual cycle (Figure 1D).

E2-mediated inhibition of $P2Y_2$-dependent ASL secretion is due to changes in E2 concentrations, not changes in ER expression levels. We isolated mRNA from primary human bronchial epithelial cultures (HBECs) and performed RT-PCR using primers directed toward ERα and ERβ. We found that ERα was equally expressed in airways from both male and female donors without CF. However, we failed to detect ERβ either by quantitative PCR (qPCR) (Figure 2A) or by

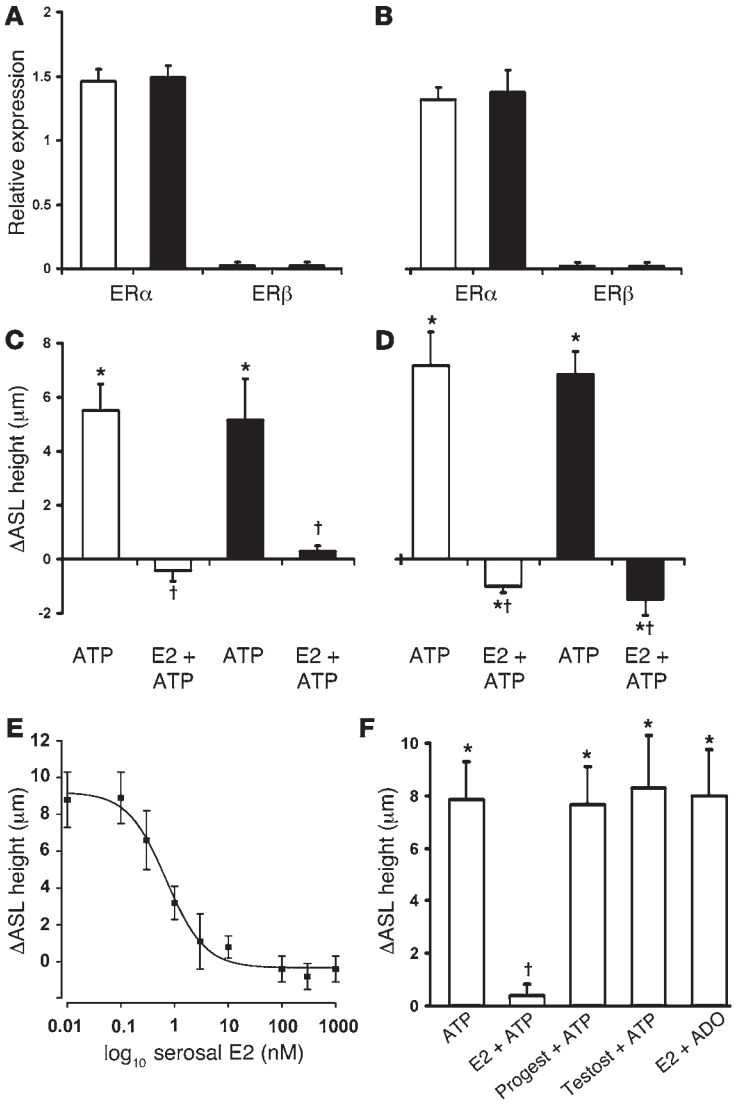

Figure 2
E2-mediated inhibition of ASL volume homeostasis is due to changes in E2 concentrations, not ER expression levels. (**A** and **B**) Real-time qPCR analysis in non-CF and CF airways, respectively, using primers directed to ERα and ERβ. For ERα, DNAs were obtained from 12 non-CF and 12 CF donors (for each, n = 6 males, white bars, and 6 females, black bars). For ERβ, cDNA was obtained from 6 non-CF and 6 CF donors (for each, n = 3 males, open bars, and 3 females, closed bars). In both cases, expression was normalized to peptidylprolyl isomerase A (PPIA). ERβ was not detectable by either standard PCR (not shown) or qPCR. (**C** and **D**) Mean non-CF and CF changes in ASL height, respectively, as measured by confocal microscopy following 100 μM ATP addition ± 10 nM serosal E2 to HBECs from male (white bars) and female donors (black bars). All n = 4. (**E**) Dose-response curve for the inhibition of ATP-mediated ASL secretion in non-CF HBECs (ΔASL height before and after 10 minutes application of 100 μM ATP) following serosal E2 addition over the range of 0.01 to 1000 nM E2 in non-CF cultures (n = 6). (**F**) ΔASL height before and after 10 minutes of 100 μM ATP or ADO addition. Hormones were added serosally at 10 nM prior to ATP/ADO addition at 10 μM. All n = 5–7. *P < 0.05 versus 0 nM E2. †P < 0.05 versus ATP alone. Progest., progesterone; testost, testosterone.

standard PCR (not shown). ERα was expressed at similar levels in males and females with CF, and ERβ was not detected (Figure 2B). We also attempted to determine whether E2 could affect glandular secretions; however, we were unable to detect ERα or ERβ cDNA in gland-derived Calu-3 cells (data not shown).

To see whether E2 inhibited ATP-mediated ASL secretion preferentially in HBECs from female as compared with male donors, we measured ASL height by confocal microscopy before and after ATP addition. Mucosal ATP addition caused an equal increase in ASL height in non-CF HBECs from both male and female donors, and acute (30 minutes) preexposure with 10 nM E2 inhibited this response (Figure 2C). Consistent with equal expression of ERα in HBECs from both male and female donors, no difference in the inhibition of ATP-mediated secretion was detected between sexes, suggesting that changing levels of E2 rather than altered ERα expression accounted for the increased inhibition of the P2 response observed in vivo (Figure 1). E2 also equally inhibited the ATP-dependent increase in ASL height in CF HBECs from male and female donors (Figure 2D).

Since there was no discernible difference in the effect of E2 on ASL secretion in males versus females, subsequent data were not separated on the basis of sex. We next measured ASL height before and after ATP addition to a group of non-CF HBECs exposed to E2 at concentrations ranging from 0.01 to 1000 nM (Figure 2E). The IC_{50} for E2 inhibition of ATP-induced ASL secretion was 0.7 nM (Figure 2E), which is close to the 50% inhibition of the UTP response observed with 0.4 nM endogenous E2 in vivo. Levels of E2 present in males or menstruating females (0.01–0.1 nM) had no effect on ASL height. However, E2 levels found in females (0.3–3 nM) inhibited ASL secretion and are commensurate with ATP-mediated ASL secretion being approximately 50% inhibited in vivo. The inhibition of P2 signaling was also specific for E2 over other sex hormones, and neither 10 nM progesterone nor 10 nM testosterone exposure had any effect on ATP-mediated ASL secretions (Figure 2F).

ADO activates CFTR via an $A2_B$ ADO receptor-dependent rise in cAMP (6). ADO addition (100 μM) also elicited a robust increase in ASL height that was unaffected by 10 nM E2 (Figure 2F). Thus, this effect appears to be specific for P2 signaling and does not appear to affect the cAMP pathway or CFTR.

Inhibition of CF ASL volume homeostasis by physiological levels of E2. We have previously utilized a system that imparts phasic shear stress to HBECs to reprise in vivo tidal breathing. This system increases ASL nucleotide levels and increases both non-CF and CF ASL height (2). We tested whether the response to phasic motion was attenuated by levels of E2 found in females (3 nM) versus males (0.1 nM) in non-CF and CF HBECs. Forty-eight hours after addition of 20 μl Ringer's solution containing Texas Red dextran, ASL height was approximately 14 and 7 μm in non-CF and CF HBECs, respectively, in the continued presence of phasic shear stress (Figure 3, A and B). As would be predicted by the dose response curve to E2 shown in Figure 2E, 0.1 nM E2 had no effect on either the non-CF or CF 48-hour response to phasic shear stress (Figure 3B). In non-CF cultures, 3 nM E2 moderately decreased ASL height,

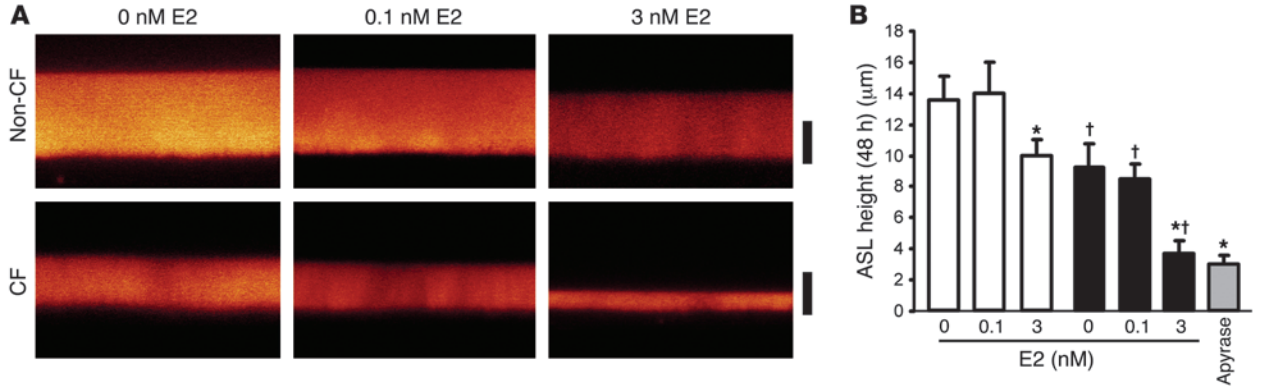

Figure 3
E2 inhibits ASL volume homeostasis in CF airways. (**A**) XZ confocal images of ASL (red) 48 hours after phasic shear stress (0.6 dynes/cm^2) in non-CF (top) and CF cultures (bottom) with 0, 0.1, or 3 nM serosal E2. (**B**) Mean data taken from **A**. White bars, non-CF HBECs (n = 6); black bars, CF HBECs (n = 5–7); gray bar, CF HBECs with 5 U/ml mucosal apyrase (n = 5). *P < 0.05 compared with 0 nM E2. †P < 0.05 compared with non-CF HBECs. Scale bars: 7 μm.

consistent with (a) the ATP system playing only a moderate role in non-CF ASL homeostasis (2) and (b) the E2-insensitive ADO/CFTR system being the main conduit for Cl^- secretion (n.b., this height [~7 μm] is predictive of the formation of a normal PCL that would still allow efficient mucus transport). In contrast, 3 nM E2 depleted CF ASL height down to approximately 3 μm. A similar decrease was observed when P2 signaling was inactivated following addition of the ATP-depleting enzyme apyrase to the ASL (Figure 3B). We also found that after 48 hours of shear stress, a 1-hour exposure to E2 in the continued presence of shear stress caused a rapid decline in both non-CF and CF ASL volume of 50% (both n = 4), suggesting that inhibition of ASL volume homeostasis would have a rapid onset after increases in blood E2 levels.

Activated ERα inhibits ATP signaling when transiently transfected into ER-null baby hamster kidney cells. To determine which ER inhibited the ATP response, we transiently transfected ER-null baby hamster kidney (BHK) cells that endogenously express $P2Y_2$ receptor ($P2Y_2$-R) with ERs tagged with monomeric orange fluorescent protein (mOr). Approximately 50% of cells per culture were successfully transfected with mOr-tagged ERs at any one time, allowing neighboring cells with and without ERs to be simultaneously imaged (Figure 4, A and B).

BHK cells displayed a robust increase in the fura-2 emission ratio following 10 μM ATP addition, which was unaffected by E2 pretreatment (Figure 4C). In contrast, neighboring cells that expressed mOr-ERα exhibited an approximately 50% reduction in fura-2 emission (i.e., Ca^{2+}_i) with 10 nM E2, suggesting that ERα can attenuate nucleotide-activated Ca^{2+} signaling (Figure 4C). The negative effect of ERα and E2 on the ATP response was abolished by addition of the ERα-specific antagonist ICI_{182780} prior to E2 addition (Figure 4D). The ATP response was unaffected by E2 in nontransfected cells or cells expressing either mOr alone or mOr-ERβ. Further, mOr-ERα only inhibited the ATP response when E2 was present, suggesting that this inhibition is specific to activated ERα (Figure 4E).

ERα does not alter $P2Y_2$-R internalization. Since ERα inhibited the ATP-mediated Ca^{2+} response, we next tested to determine whether this effect was due to ERα-induced removal of a P2-R from the plasma membrane prior to purine stimulation. Since there are no good antibodies against P2 receptors, we utilized a $P2Y_2$-R construct with an external HA epitope tag and tested to determine whether HA–$P2Y_2$-R surface expression was altered by ERα/E2 exposure in BHK cells (Figure 5). HA–$P2Y_2$-R could clearly be identified at the cell surface (Figure 5A). A 30-minute incubation with 10 nM E2 had no effect on the localization of the receptor (Figure 5B), and the receptor could be seen to internalize following stimulation with 10 μM ATP, as evidenced by the appearance of intracellular punctae (Figure 5C). This protocol was repeated when HA–$P2Y_2$-R was coexpressed with mOr-ERα (Figure 5, D–F). Neither expression nor activation of ERα had any effect on HA–$P2Y_2$-R surface expression or ATP-stimulated internalization of the receptor (Figure 5G).

E2-dependent inhibition of Cl^- secretion is due to altered Ca^{2+} signaling rather than altered Cl^- channel properties. To search for the mechanism whereby E2 inhibited ATP-mediated ASL secretion, we examined multiple facets of the P2 pathway in airway epithelia. We first microsampled ASL from non-CF HBECs and measured the ASL ATP levels by luminometry. An addition of 10 nM serosal E2 did not affect endogenous ASL ATP levels over 1 hour (vehicle, 16.8 ± 2.1 nM; E2, 14.9 ± 3.8 nM; both n = 6).

To test whether the inhibition of airway Ca^{2+} signaling seen in BHK cells (Figure 4) was specific for a particular P2 receptor, we next measured changes in the fura-2 emission ratio in non-CF HBECs following either ATP or UDP addition, which stimulates P2X/$P2Y_2$-R or $P2Y_6$-R, respectively. The peak fura-2 response was depressed after addition of both agonists, suggesting that E2 inhibits a crucial step in Ca^{2+} signaling that is downstream of the P2-R (Figure 6A). The IC_{50} for this inhibition was 2.4 nM (Figure 6B). This inhibition was abolished by pretreatment with the ER antagonist ICI_{182780} (n = 4; data not shown), indicating that we were imaging an ERα-dependent event.

We next determined whether G_q/PLC-dependent inositol phosphate (IP) formation was altered by E2 exposure. Due to the greater number of cells required for these experiments, we utilized an immortalized CF nasal cell line (JME cells) that can be grown at greater densities than HBECs. The ATP-stimulated fura-2 response was also inhibited in JME cells in a dose-dependent fashion, suggesting that they were a suitable model for further study (Figure 6B). Confluent JME cells passaged at the same time as the cells used for the fura-2 experiments in Figure 6B were labeled with [^{3}H]myoinositol phosphate, and a 10 μM ATP addition caused a

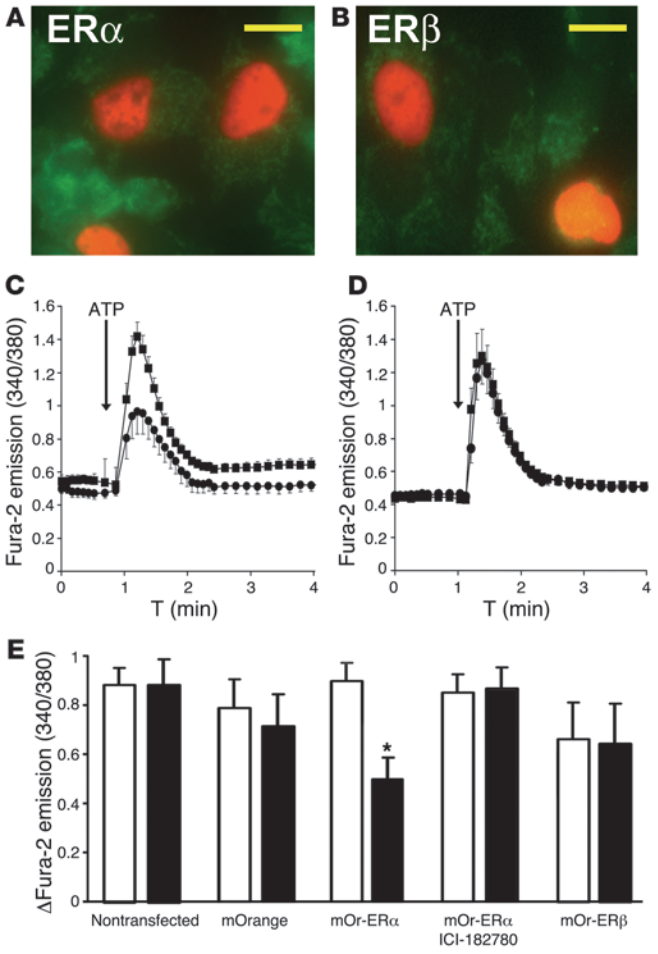

Figure 4
Transient expression of ERα but not ERβ inhibits ATP-dependent increases in intracellular Ca^{2+} when activated by E2 in BHK cultures. (**A** and **B**) Images of fura-2–loaded BHK cells (green) expressing either ERα or ERβ, respectively, linked to mOr. (**C**) Mean fura-2 emission ratio over time simultaneously imaged in nontransfected BHK cells (squares) and neighboring cells expressing mOr-ERα (circles) following a 10-minute pretreatment with 10 nM E2, then a 10 μM ATP addition (n = 7). (**D**) Mean fura-2 emission ratio over time simultaneously imaged in nontransfected BHK cells (squares) and mOr-ERα–expressing cells (circles) (n = 9) following a 30-minute pretreatment with ICI_{182780}, then 10 minutes with 10 nM E2 followed by a 10 μM ATP addition. (**E**) Mean ATP-induced changes in fura-2 emission without (white bars) and with (black bars) 10 nM E2 in nontransfected cells (n = 6) and following transfection with mOr (n = 3), mOr-ERα (n = 7), mOr-ERα in the presence of ICI_{182780} (n = 7), and mOr-ERβ (n = 5). *P < 0.05 compared with control. Scale bars: 10 μm.

robust increase in [^{3}H]IP levels that was not altered by a 15-minute 10 nM E2 exposure, indicating that G_q/PLC activity and IP production are E2-insensitive (Figure 6C).

Thapsigargin is a sarcoplasmic/endoplasmic reticulum Ca^{2+}-ATPase (SERCA) pump inhibitor that allows Ca^{2+} to leak out of the endoplasmic reticulum rather than being recycled (22). We first removed Ca^{2+} from the bathing solution to prevent confounding Ca^{2+} influx (23), and under these conditions, the thapsigargin-induced fura-2 response was not altered by E2 (Figure 6D).

We next determined the effects of E2 on Ca^{2+} influx. With 2 mM Ca^{2+} in the external bath solution (standard Ringer's solution), 10 nM E2 induced a robust inhibition of the ATP fura-2 response (Figure 6E). Removal and chelation of external Ca^{2+} reduced both the peak and plateau of the ATP-induced fura-2 response by approximately 50%, indicating that approximately 50% of Ca^{2+} enters airway epithelial cells from the extracellular environment following ATP addition (Figure 6F). In the presence of zero $Ca^{2+}{}_o$, E2 had no further effect, confirming that Ca^{2+} influx is reduced by E2 exposure (Figure 6F).

To determine whether E2 also acted downstream of Ca^{2+} signaling, we measured UTP-dependent short-circuit current (I_{sc}) in non-CF HBECs. UTP and ATP are equally efficacious in activating $P2Y_2$-R (24). However, in this case, we used UTP because ATP can be metabolized to ADO by ecto-ATPases (4), which may activate CFTR and obfuscate Ca^{2+}-dependent changes in I_{SC} (25). HBECs mounted in Ussing chambers were treated with amiloride and subsequently exposed to either UTP to activate the $P2Y_2$ pathway or ionomycin to bypass the $P2Y_2$ pathway and directly increase $Ca^{2+}{}_i$ (Figure 6G). While the UTP response was significantly inhibited by E2, the ionomycin response was unaffected, indicating that E2 does not alter intrinsic Cl^- secretion and rather affects upstream Ca^{2+} signaling (Figure 6G).

Potentiation of nucleotide-dependent ASL volume homeostasis by tamoxifen. Since E2 caused an inhibition of ATP-mediated ASL secretion, we hypothesized that this inhibition could be reversed by ER antagonists. To test this hypothesis, we measured the fura-2 emission ratio in JME cells following ATP addition and after exposure to ER antagonists (Figure 7A). The ATP-induced increase in the fura-2 ratio was reduced by acute E2 addition and restored by the addition of the ER antagonist ICI_{182780} (1 μM) with E2 (Figure 7A). Interestingly, tamoxifen (TXN) increased the Δfura-2 ratio after ATP addition to twice the level of ATP alone, suggesting that TXN potentiates the $P2Y_2$ response (Figure 7A).

Since the fura-2 response was enhanced by TXN, we next determined whether this compound could increase ATP-induced ASL secretion in non-CF and CF HBECs. As would be predicted by the increase in fura-2 emission shown in Figure 7A, TXN potentiated ATP-induced ASL secretion, leading to an increase in both magnitude and duration of ASL volume secretion in non-CF and CF cultures compared with ATP alone (Figure 7, B and C). The TXN-induced potentiation of the ATP response persisted in the presence of 10 nM E2, suggesting that TXN may be efficacious in reversing the inhibition of ASL volume homeostasis seen during high–E2 level days (Figure 7, B and C).

Since ATP is endogenously secreted into the ASL (4), we next determined whether TXN alone could stimulate ASL secretion. TXN alone had no effect on non-CF or CF ASL ATP levels (non-CF ASL ATP: 30 minutes vehicle, 15.8 ± 3.4 nM; 30 minutes TXN, 12.3 ± 1.9 nM; both n = 6; CF ASL ATP: 30 minutes vehicle, 13.3 ± 0.8 nM; 30 minutes TXN, 17.5 ± 2.6 nM; both n = 5). We then added 200 μM TXN with no exogenous ATP mucosally to non-CF and CF cultures (Figure 7D). TXN addition caused a sustained increase in ASL height in both non-CF and CF HBECs, which persisted for over 1 hour (Figure 7D). This response was less than the change in ASL height seen with ATP and TXN in Figure 7, B and C, perhaps since endogenous ATP levels are much smaller than can be delivered pharmacologically (i.e. <100 nM vs. 100 μM) (4). Importantly, TXN reversed the decline in ASL height seen in untreated CF HBECs and caused ASL height

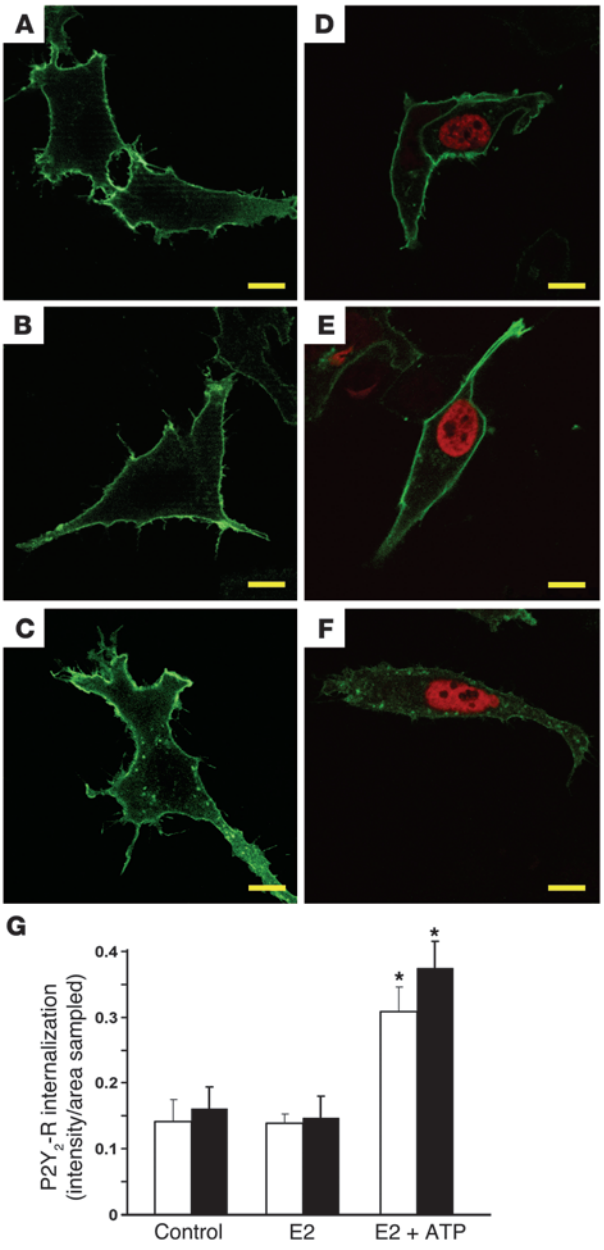

Figure 5
E2 does not induce $P2Y_2$-R internalization. BHK cells were transfected with HA-tagged $P2Y_2$-R (green) ± mOr-ERα (red) and fixed in PFA after E2/ATP addition. (**A**–**C**) Sequential images of HA–$P2Y_2$-R before E2 addition, 30 minutes after 10 nM E2 exposure, and 30 minutes after the addition of 100 μM ATP in the presence of E2, respectively. (**D**–**F**) $P2Y_2$-R cotransfected with mOr-ERα before and after 30-minute 10 nM E2 exposure and 30 minutes after the addition of 100 μM ATP in the presence of E2. (**G**) Bar graph quantifying HA–$P2Y_2$-R internalization to the area measured. White bars, HA–$P2Y_2$-R alone; black bars, HA–$P2Y_2$-R and ERα. Data are from transfections performed on 3 separate occasions. Scale bars: 10 μm. *$P < 0.05$ versus E2 alone.

to increase to a value that was suitable for mucus clearance (~15 μm) as compared with less than 5 μm in the non-TXN group (Figure 7D). Pretreatment of CF HBECs with 2 U/ml mucosal apyrase inhibited this response. After 1 hour of TXN exposure with apyrase, ASL height was 6.0 ± 0.7 μm ($n = 7$) compared with 16.5 μm ASL height shown in Figure 7D for CF HBECs with TXN alone. That this change was due to an increase in Cl^- secretion was confirmed by pretreatment with bumetanide, which abolished the TXN-induced increase in ASL height in both non-CF and CF ASL (Figure 7D).

Discussion

The effect of the menstrual cycle on in vivo nasal PDs. We have speculated that a putative female disadvantage with respect to the progression of CF lung disease in part reflects a reduced ability of females with CF to activate Cl^- secretion and adequately hydrate their airways. As a first step toward testing this hypothesis, we measured in vivo nasal PDs in regularly cycling females with and without CF, which we correlated with changes in blood estrogen levels. In agreement with Sweezey et al. (26), we did not detect cyclical changes in the amiloride-sensitive nasal PD (Figure 1, D and H), nor did we detect a cyclic change in the ISO response, which represents activation of CFTR in subjects without CF (Figure 1D). However, we found that the UTP-mediated Cl^- secretory response varied by approximately 50% in subjects both with and without CF during the menstrual cycle (Figure 1), which correlated with a 4-fold change in blood E2 levels. The timing of the second PD (Figure 1, B and F) was designed to increase the likelihood of performing the measurement on a high–E2 level day but not necessarily the peak day(s), and it appears that the second recording was largely performed before the preovulatory estrogen maxima, since the average E2 level was approximately 30%–50% of the expected peak E2 level. Thus, the effects of E2 on Cl^- secretion in cycling women may be even higher during the preovulatory estrogen maxima. Sampling later in the cycle was avoided, since the well-recognized variability in follicular phase when estrogen falls and progesterone rises could easily lead to increased variability in nasal PD recordings, although no effects of progesterone were seen in vitro (Figure 2F), which suggests that the relatively high concentrations of E2 alone are sufficient to impair Cl^- secretion.

Is there a sex-related difference in CF? Whether or not sex is a risk factor in CF remains somewhat contentious. In 1992, based on a cohort of 633 patients, Kerem et al. (27) reported that being female was associated with significantly decreased rates of survival in CF patients awaiting lung transplantation. Based on a cohort of 848 subjects with CF, Demko et al. (13) reported that females with CF exhibited an increased rate of decline in lung function and a reduced survival rate compared with their male counterparts and also tended to acquire mucoid *P. aeruginosa* earlier than males. A larger multicenter study with more than 20,000 patients found that females with CF under the age of 20 were 60% more likely to die than males with CF (15). Outside this age bracket, sexual phenotype was not a significant risk factor, although in 1999 the median survival age was 25.3 for females with CF and 28.4 for males with CF. Recently, Verma et al. (28) suggested that the sex-related difference in survival may have diminished or even been mitigated with better physical therapy, more aggressive antibiotics, and improved care after lung transplants. It is noteworthy that even in 2006, females with CF still scored worse than males with CF in a health-related quality of life study (29) and, importantly, were significantly more prone to acute exacerbations than males with CF (14).

We propose that a better understanding of sex-related differences in innate lung defense may produce targeted therapeutic

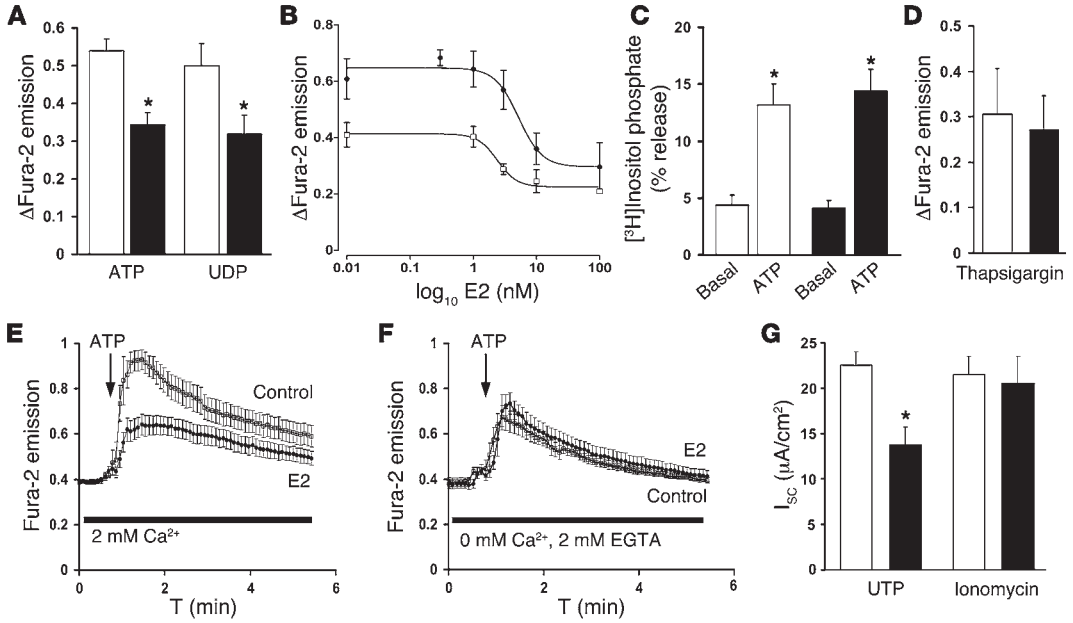

Figure 6

E2 inhibits Ca^{2+} influx in airway epithelia. Non-CF HBECs and JME CF cells were incubated with vehicle (white bars) or 10 nM E2 (black bars) unless otherwise specified. (**A**) Mean changes in fura-2 emission ratio in HBECs exposed to ATP (10 μM) or UDP (1 mM) ± E2 (both $n = 6$). (**B**) Mean changes in fura-2 emission ratio (340/380 nm) in non-CF HBECs (open symbols; $n = 6$) and CF JME cells (closed symbols; $n = 4$–6) exposed to 0.01–100 nM serosal E2 followed by 10 μM mucosal ATP. (**C**) [^{3}H]IP release from JME cells before and after 10 μM ATP addition ± E2. (**D**) Mean changes in fura-2 emission ratio following 1 μM thapsigargin addition ± E2 to JME cells in a modified Ringer bath solution with 0 mM Ca^{2+} and 2 mM EGTA (all $n = 6$). (**E**) Mean change in fura-2 emission over time following 10 μM ATP addition in JME cells ± E2 with 2 mM external Ca^{2+} ($n = 9$). (**F**) Fura-2 emission over time following 10 μM ATP addition in JME cells ± E2 with 0 Ca^{2+} and 2 mM EGTA ($n = 9$). (**G**) Mean I_{SC} in non-CF HBECs ± E2 (10 nM). I_{sc} was measured following mucosal amiloride (100 μM) treatment, after which Cl^- secretion was elicited either with UTP (100 μM) or ionomycin (1 μM) (all $n = 16$). *$P < 0.05$ compared with control.

approaches to specifically attenuate the severity of lung disease in women with CF. Reduction of airway secretion hydration is one clear adverse effect of estrogens on female innate immunity. Estrogens have other potential dampening effects on innate immunity, including E2-mediated inhibition of TLR signaling (30).

Airway ER expression patterns. In agreement with previous reports (31), we found that ERα was expressed at similar levels in males compared with females and ATP-mediated ASL secretion was equally inhibited cultures derived from both males and females (Figure 2). Thus, it is likely that E2-linked sex-related differences in CF are due to circulating E2 levels rather than male versus female ERα expression levels. However, there remains the perplexing question of why ERs are expressed in the airways and why they regulate nucleotide-activated Cl^- secretion. Data are emerging that show females are also more prone than males to lung cancer, which has been linked to E2, suggesting that ERs are involved in cell turnover in the lung (32). Clearly, further studies are required to understand the function of ERs in the airways and why they can regulate Ca^{2+} signaling.

Do ERs directly alter Ca^{2+}_i signaling in airway epithelia? While some studies in reproductive tissues have demonstrated a direct stimulation of Ca^{2+}_i by E2 (33, 34), other studies using nonreproductive tissues have demonstrated an apparent E2-mediated suppression of the purinergic response: Knight and Burnstock (35) demonstrated that P2X-mediated bladder contractions were attenuated by increased E2 during the rat estrous cycle, and Chaban and coworkers (36, 37) have shown that ATP-mediated Ca^{2+} signaling was inhibited following activation of ERα in murine dorsal root ganglion cells. Similarly, we did not find any significant change in Ca^{2+}_i following E2 addition in either primary HBECs or a CF nasal epithelial cell line (Figure 6). We also failed to detect any increase in IP levels following E2 addition in JME cells (Figure 6), and we found that ERα-expressing BHK cells were unable to mobilize an appropriate Ca^{2+} response once ERα was activated (Figure 4). Thus, it is possible that the "wiring" between ERs and the Ca^{2+} mobilization apparatus is different in reproductive versus other tissues.

Mechanism of interaction between E2 and the $P2Y_2$ cascade. We tested to determine whether the presence and/or activation of ERα could decrease the level of $P2Y_2$-R in the plasma membrane, which could potentially reduce the amount of receptor available to be activated by its ligand. As shown in Figure 5, E2 had no effect on $P2Y_2$-R surface expression, and ATP-stimulated internalization was likewise unaffected, suggesting that the $P2Y_2$-R functions normally in the presence of ERα. Similarly, we also found that ATP release was not altered by E2 exposure. We have focused our attention on $P2Y_2$-R, since the UTP response is inhibited in vivo (Figure 1). However, the in vitro ATP response was also E2 sensitive, and both $P2Y_2$-R and P2X-R are stimulated with ATP (38, 39). We also found that E2 not only inhibited the ATP/UTP responses but also inhibited the UDP-stimulated $P2Y_6$-R response (Figure 6A), so it is likely that E2 affects multiple P2-Rs.

Following activation of G_q, PLC is activated and forms IP_3, which in turn stimulates Ca^{2+} release from the endoplasmic reticulum. However, we failed to observe any difference in IP formation after ATP exposure, suggesting that G_q/PLC are unaffected by E2

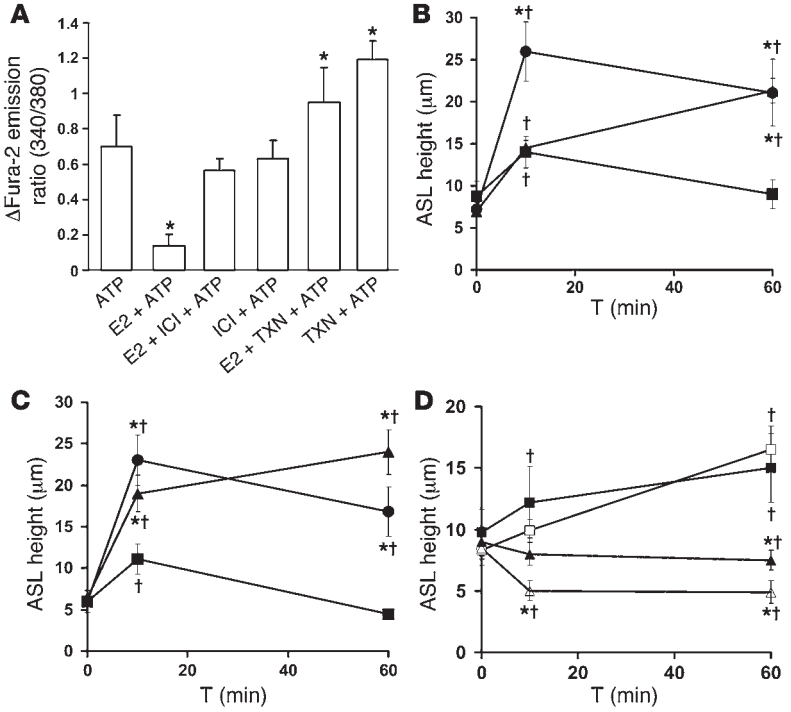

Figure 7
Antiestrogens reverse the adverse effects of E2 on ASL volume homeostasis. (**A**) Mean change in fura-2 emission ratio in JME cells exposed to ATP (10 μM) and vehicle or ATP and either 10 nM E2, E2 and 1 μM ICI_{182780}, ICI_{182780}, E2 with 10 μM TXN, and ICI_{182780}, or 10 μM TXN. All $n = 6$. (**B** and **C**) ASL height measured by XZ confocal microscopy in non-CF and CF HBECs, respectively. 200 μM mucosal ATP addition (squares); 200 μM mucosal ATP and 200 μM mucosal TXN (circles); 200 μM mucosal ATP and 200 μM mucosal TXN and 10 nM serosal E2 (triangles). (**D**) ASL height over time in non-CF (closed symbols) and CF (open symbols) HBECs with TXN ± bumetanide. Squares, 200 μM mucosal TXN; triangles, 200 μM mucosal TXN and 10 μM serosal bumetanide. All data shown as mean ± SEM. *$P < 0.05$ compared with ATP or TXN alone. †$P < 0.05$ versus 0 minutes.

(Figure 6C) even though cells from the same passage displayed a reduced fura-2 response with E2 (Figure 6B).

Thapsigargin increases Ca^{2+} leak into the cytoplasm by inhibiting Ca^{2+} uptake into the endoplasmic reticulum (22). We found that the amount of $Ca^{2+}{}_i$ released following thapsigargin addition was not altered by E2 exposure (Figure 6D), suggesting that the Ca^{2+} stores are not E2 sensitive. Once $Ca^{2+}{}_i$ is released from intracellular stores, it often stimulates Ca^{2+} influx from outside the cell. By switching between high and nominally zero Ca^{2+} in the external bath, it is possible to differentiate between store Ca^{2+} versus Ca^{2+} influx from the extracellular environment. With external Ca^{2+}, ATP addition stimulated a robust increase in the fura-2 ratio (Figure 6E). Removal of extracellular Ca^{2+} approximately 60 seconds before ATP addition decreased both the peak and plateau phases of the fura-2 response (Figure 6F). Importantly, we found that the portion of the Ca^{2+} response that was due to Ca^{2+} entry was E2 sensitive (Figure 6F). However, the nature of the interaction between the Ca^{2+} influx pathway and ERα remains to be determined.

When airway epithelia are mounted in Ussing chambers, mucosal ATP or UTP addition results in a transient increase in I_{sc} that is typical of nucleotide-activated Cl^- secretion. While UTP-mediated I_{sc} was diminished by E2 pretreatment, I_{sc} was not affected by E2 following the addition of the Ca^{2+} ionophore ionomycin, indicating that E2 does not affect Cl^- secretion directly but rather affects upstream signaling (Figure 6G). The genetic identity of the ATP-activated Cl^- channel(s) is unknown. However, candidates for this unidentified Cl^- channel include bestrophin (40), the outwardly rectifying Cl^- channel (ORCC) (41), and TMEM16A (42, 43). Our study does not differentiate between these channels. However, it is likely that this unidentified channel is not directly affected by E2 but rather that its upstream second messenger, i.e., Ca^{2+}, is E2 sensitive.

The impact of estrogen on CF ASL volume homeostasis. We hypothesized that CF airways are more vulnerable to catastrophic events that may disrupt ASL homeostasis. For example, acute infection with a common airway pathogen (respiratory syncytial virus) upregulates extracellular ATPases and depletes the ASL of ATP, preventing activation of $P2Y_2$-R (2). This infection does not abolish normal ASL volume homeostasis, since non-CF airways can still secrete via ADO-mediated activation of CFTR. However, CF cultures are dramatically affected, and they lose the ability to respond to phasic shear stress, which results in a depletion of PCL volume. Extending this hypothesis, we propose that another such "insult" is high circulating E2. We predict that female CF patients would have rates of mucus transport comparable to those of male CF patients for approximately 3 weeks per month but that when E2 levels increased sufficiently to inhibit ATP-mediated Cl^- secretion, these patients would have significantly reduced mucociliary clearance, leaving them less able to clear airborne pathogens then males with CF or females without CF. Addition of E2 for 1 hour was sufficient to reduce CF ASL volume by 50% under phasic shear stress conditions, suggesting that reductions in ASL volume may occur quite rapidly once E2 begins to rise.

In regularly cycling females with CF, periods of high estrogen represent a risk period for acute exacerbations. If these patients do not experience an acute exacerbation during this risk period, then there will be no observable difference between them and males with CF. However, there is a 1 in 4 chance that they will experience an acute exacerbation during the risk period, and if they do, they will be less able to clear inhaled pathogens, which may lead to greater intensity and duration of infection. Wang et al. demonstrated that the frequency of viral respiratory infection was closely associated with pulmonary deterioration in CF patients (44). Interestingly, Block et al. (14) reported that adult females with CF are more likely to experience acute exacerbation than males with CF, although whether E2-mediated inhibition of airway ion transport described in this paper is contributory to this increased rate of infection remains to be tested.

Implications for the treatment of CF. Our data indicate that the effects of E2 can be blocked by the ER antagonist ICI_{182780}. This compound is approved for human use and may benefit females with CF by abrogating the negative effects of E2. We also tested the effects of TXN on Ca^{2+} signaling and ASL secretion. While ICI_{182780} is a pure antiestrogen, TXN is classed as a selective ER modulator or SERM that has mixed agonist/antagonist capabilities (45). Surprisingly, TXN actually potentiated the effect of ATP on ASL secretion in both non-CF and CF cultures, even in the presence of 10 nM E2 (Figure 7). This suggests that SERMs may be preferable to pure antiestrogens in treating CF lung disease.

In conclusion, we have shown that physiological elevations in estrogen (E2) that occur prior to ovulation in vivo are associated with an inhibition of UTP-mediated Cl^- secretion in females with CF. In vitro, we have demonstrated that this inhibition is due to concentration-dependent changes in E2 rather than male versus female ER expression levels and is induced by an ERα-mediated inhibition in Ca^{2+} influx rather than altered IP formation or a direct effect on the ion channel. We hypothesize that this inhibition of Cl^- secretion leaves females with CF with reduced mucus clearance for approximately 1 week per month, which contributes to increased susceptibility to acute exacerbations and sex inequality in CF lung disease. Finally, we propose that antiestrogen therapies using existing, clinically available compounds may be beneficial in the treatment of CF lung disease.

Methods

Study subjects. All subjects experienced regular menstrual cycles and were not using hormonal contraceptives or inhaling steroids at the time of investigation. Mean ages were 30.9 ± 1.9 years (n = 12) for subjects without CF and 30.3 ± 2.1 years (n = 10) for subjects with CF. Mean CF forced expiratory volume in 1 second (FEV_1) (% predicted) was 50.2 ± 6.2 (n = 10). Five patients were homozygous for ΔF508, 2 patients carried 1 copy of ΔF508 with an unidentified mutation on the other allele, 1 patient carried 1 copy of ΔF508 and 1 copy of R117H, 1 patient carried 1 copy of ΔF508 and 1 copy of 2789+5G→A, and 1 patient carried 1 copy of 1717-1G→A and 1 copy of N1303K.

In vivo nasal PDs. The study protocol was approved by the University of North Carolina (UNC) Committee on the Protection of Rights of Human Subjects, and written informed consent was obtained. Subjects were asked to identify the first day of their last menstrual period to allow assignment of likely cycle phase. PD was measured between a subcutaneous reference electrode and an exploring electrode placed against the inferior turbinate as previously described (46). In brief, electrodes were connected via calomel half-cells to a high-impedance voltmeter electrically isolated from the subject. The modified exploring (nasal) catheter was designed with a single lumen catheter (3 cm length of polyethylene 10 tubing threaded over a 30-gauge needle) that acts as a flowing bridge. Four perfusion lines (polyethylene 50 tubing; BD) were connected to the perfusion catheter (identical polyethylene tubing).

Tissue procurement and cell culture. Human excess donor lungs and excised recipient lungs were obtained at the time of lung transplantation from portions of main stem or lumbar bronchi, and cells were harvested by enzymatic digestion as previously described under a protocol approved by the UNC Institutional Review Board (47). HBECs were maintained at an air-liquid interface in a modified bronchial epithelial growth medium (BEGM) medium with 5% CO_2 at 37°C and used 2–5 weeks after seeding on 12-mm Transwell permeable supports (Corning) coated with human placental type VI collagen (Sigma-Aldrich).

BHK cells were cultured in DMEM/F12 medium containing 5% FBS at 37°C in 5% CO_2 on glass slides for imaging or 12-well plastic plates for biochemical experiments. The absence of ERα and ERβ was confirmed by PCR (data not shown). Cultures that were approximately 75% confluent were transfected for 4-6 hours using Effectene reagents (QIAGEN) per the manufacturer's instructions. Cells were then allowed to incubate for 24 hours before use. We recorded fura-2 emission before and after photobleaching mOr to confirm that mOr did not alter the fura-2 signal (n = 4). mOr was provided by Roger Tsien (Department of Pharmacology, UCSD, San Diego, California, USA), while ERα and ERβ were provided by Richard Day (Department of Medicine, University of Virginia, Charlottesville, Virginia, USA) and Kenneth Korach (Laboratory of Reproductive and Developmental Toxicology, National Institute of Environmental Health Sciences, Research Triangle Park, North Carolina, USA), respectively. HA–$P2Y_2$-R was donated by Kendall Harden (Department of Pharmacology, UNC, Chapel Hill, North Carolina, USA).

CF nasal epithelial (JME/CF15) cells are homozygous for ΔF508 CFTR and polarize when grown on filters (48). The culture medium contained DMEM/F-12 with 10% FBS, 2 mM L-glutamine, 100 U/ml penicillin, 100 mg/ml streptomycin, 10 ng/ml epidermal growth factor, 1 μM hydrocortisone, 5 mg/ml insulin, 5 μg/ml transferrin, 30 nM triiodothyronine, 180 μM adenine, and 5.5 μM epinephrine at 37°C in 5% CO_2.

PCR analysis. RNA was extracted using the standard protocol from the RNeasy Mini Kit (QIAGEN). The RNA was quantified by spectrometry, and a known quantity of RNA was used to make cDNA using SuperScript II (Invitrogen) and random primers. RT-PCR was performed using the Roche LightCycler system. The reactions were incubated at 95°C for 10 minutes followed by 95°C for 0 seconds, 55°C for 5 seconds, and 72°C for 8 seconds for 45 cycles with a single fluorescence detection point at the end of the relevant annealing or extension segment.

Primer sequences. The gene-specific primer sequences used for qPCR were as follows (5′ to 3′): ERα: forward, TGCCAAGGAGACTCGCTACT, and reverse, CTGGCGCTTGTGTTTCAAC; and ERβ: forward, TCAGCTTGTGACCTCTGTGG, and reverse, TGTATGACCTGCTGCTGGAG.

Confocal microscopy. To label ASL, Ringer's solution containing Texas Red dextran was added to HBEC mucosal surfaces. Perfluorocarbon (PFC) was added mucosally to prevent ASL evaporation, and the cultures were imaged using a Leica SP5 confocal microscope with a ×63 glycerol immersion objective. Five points per culture were scanned and an average ASL height determined using ImageJ (http://rsbweb.nih.gov/ij/). Nucleotides were added to mucosal surfaces as dry powders in PFC at approximately 200 μM (2). We accelerated/decelerated the HBECs inside a highly humidified incubator to generate 0.5 dyne/cm^2 apical shear stress at culture surfaces as previously reported (2).

For labeling of plasma membrane HA–$P2Y_2$-R, BHK cells grown on glass coverslips were precooled on ice for 10 minutes before being labeled for 45 minutes with anti-HA monoclonal antibodies in PBS. Cells were washed 3 times with ice-cold PBS to remove the antibodies and then warmed to 37°C and treated with ATP with or without E2. The experiment was stopped at different times by fixing the cultures with 4% PFA (for 10 minutes at 21°C). After washing 3 times in PBS, cells were blocked with 1% BSA and 5% normal goat serum (NGS) before addition of secondary antibody for 1 hour. To quantify HA–$P2Y_2$-R internalization, 10 regions of interest were drawn inside the cytoplasm of each cell, which approximated 10% of total cell area and which excluded the space occupied by the nucleus. The intensity of HA–$P2Y_2$-R was normalized to the area of the region of interest sampled using ImageJ.

Measurement of PCL ATP concentrations. 25 μl PBS was placed on HBEC surfaces, and 5–10 μl PCL was sampled by microcapillary pipettes using a micromanipulator. ATP was then measured by luminometry (2).

Measurements of Ca^{2+}_i. Cultures were loaded with fura-2–AM (5 μM at 37°C for 40 minutes) and imaged with a ×40 oil objective on a Nikon TE300

microscope outfitted with an Orca camera (Hamamatsu), and fluorescence was acquired alternately at 340 and 380 nm (emission >450 nm). In all cases, background light was measured and subtracted by exposing cells to digitonin (15 μM) and $MnCl_2$ (10 mM) as previously described (47).

Measurement of IPs. HBECs were labeled for 18 hours in inositol-free DMEM containing 4.5 g/l glucose and 2 μCi/ml [^{3}H]inositol. For 20 minutes prior to study, cultures were placed in serum-free medium containing 10 μM lithium and [^{3}H]inositol and challenged with E2 for 15 minutes followed by ATP for an additional 15-minute period. No changes in medium were made subsequent to [^{3}H]myoinositol addition to avoid release of endogenous ATP from stressed cells. Incubations were terminated by the addition of 5% ice-cold formic acid, and the formic acid extracts were neutralized by extractions with ethyl ether. The resultant [^{3}H]IPs were separated on Dowex AG1-X8 columns as described previously (49). Radioactivity was determined using a TopCount Microplate Liquid Scintillation Counter (PerkinElmer). The levels of ^{3}H-labeled IPs were normalized to total membrane [^{3}H]IP levels as previously described (49).

Ussing chambers. I_{sc} and resistance (R_t) were measured in HBECs mounted in Ussing chambers (Physiologic Instruments) and were bathed bilaterally with Krebs-Ringer bicarbonate (KRB) (37° C, pH 7.4) circulated by gas lifts (95% O_2/5% CO_2) as reported (47). To eliminate the contribution of apical Na^+ channels and measure Cl^- secretion, amiloride (10^{-4} M) was added to the mucosal bath, followed by forskolin and UTP.

Solutions and chemicals. Ringer solution for NPD measurements contained 115 mM NaCl, 25 mM $NaHCO_3$, 2.4 mM K_2HPO_4, 0.4 mM KH_2PO_4, 1.2 mM $CaCl_2$, and 1.2 mM $MgCl_2$, pH 7.4. A low Cl^- Ringer solution where NaCl was replaced with 115 mM NaGluconate was also used. For confocal microscopy and Ca^{2+} experiments, cultures were bathed serosally in a modified Ringer solution containing 116 mM NaCl, 10 mM $NaHCO_3$, 5.1 mM KCl, 1.2 mM $CaCl_2$, 1.2 mM $MgCl_2$, 20 mM TES, and 10 mM glucose, pH 7.4. All Ussing chamber experiments were performed in Krebs-Ringer bicarbonate solution, pH 7.4, containing 120 mM NaCl, 5.2 mM KCl, 1.2 mM $CaCl_2$, 1.2 mM $MgCl_2$, 2.4 mM $NaHPO_4$, 0.4 mM NaH_2PO_4, 25 mM $NaHCO_3$, and 5 mM glucose. PBS was used as an apical volume challenge and for washing the apical surface.

Fura-2–AM, FITC and Texas Red dextrans, and Alexa Fluor 488 antibodies were obtained from Invitrogen. ADO, apyrase, ATP, digitonin, E2, progesterone, TXN, testosterone, thapsigargin, UTP, and all salts and buffers were obtained from Sigma-Aldrich. ICI_{182780} was purchased from Tocris Bioscience. PFC (FC-77) was obtained from 3M and had no effect on ASL height, as previously reported (50). ADO and ATP were added as dry powder suspended in PFC (FC-77) to result in a final concentration of approximately 300 μM. When used, aprotinin was added at 1 unit/ml in the initial wash of Ringer's solution with the Texas Red dextran.

Statistics. All data are presented as the mean ± SEM for *n* experiments. Differences between means were tested for statistical significance using paired or unpaired *t* tests or Wilcoxon rank-sum or Mann-Whitney *U* tests as appropriate. From such comparisons, differences yielding $P \leq 0.05$ were judged to be significant. HBECs derived from 3 or more donors were used for each experiment, and experiments using cell lines were repeated on 3 separate occasions.

Acknowledgments

We gratefully acknowledge the technical assistance of Hadley Hartwell and Michael Watson and thank Richard Boucher for critical reading of the manuscript. This work was funded by Cystic Fibrosis Foundation grant TARRAN06I0 and NIH grants R01 HL074158, P50 HL084934, and U54HD035041-11.

Received for publication September 11, 2007, and accepted in revised form September 24, 2008.

Address correspondence to: Robert Tarran, Cystic Fibrosis/Pulmonary Research and Treatment Center, 7125 Thurston-Bowles Building, CB 7248, University of North Carolina, Chapel Hill, North Carolina 27599, USA. Phone: (919) 966-7052; Fax: (919) 966-5178; E-mail: robert_tarran@med.unc.edu.

Ray D. Coakley, Hengrui Sun, and Lucy A. Clunes contributed equally to this work.

1. Knowles, M.R., and Boucher, R.C. 2002. Mucus clearance as a primary innate defense mechanism for mammalian airways. *J. Clin. Invest.* **109**:571–577.
2. Tarran, R., et al. 2005. Normal and cystic fibrosis airway surface liquid homeostasis. The effects of phasic shear stress and viral infections. *J. Biol. Chem.* **280**:35751–35759.
3. Danahay, H., and Jackson, A.D. 2005. Epithelial mucus-hypersecretion and respiratory disease. *Curr. Drug Targets Inflamm. Allergy.* **4**:651–664.
4. Lazarowski, E.R., et al. 2004. Nucleotide release provides a mechanism for airway surface liquid homeostasis. *J. Biol. Chem.* **279**:36855–36864.
5. Kunzelmann, K., and Mall, M. 2003. Pharmacotherapy of the ion transport defect in cystic fibrosis: role of purinergic receptor agonists and other potential therapeutics. *Am. J. Respir. Med.* **2**:299–309.
6. Rollins, B.M., et al. 2008. A2B adenosine receptors regulate the mucus clearance component of the lung's innate defense system. *Am. J. Respir. Cell Mol. Biol.* **39**:190–197.
7. Tarran, R., Button, B., and Boucher, R.C. 2006. Regulation of normal and cystic fibrosis airway surface liquid volume by phasic shear stress. *Annu. Rev. Physiol.* **68**:543–561.
8. Chmiel, J.F., and Davis, P.B. 2003. State of the art: why do the lungs of patients with cystic fibrosis become infected and why can't they clear the infection? *Respir. Res.* **4**:8.
9. Gibson, R.L., Burns, J.L., and Ramsey, B.W. 2003. Pathophysiology and management of pulmonary infections in cystic fibrosis. *Am. J. Respir. Crit. Care Med.* **168**:918–951.
10. Hersh, C.P., et al. 2004. Predictors of survival in severe, early onset COPD. *Chest.* **126**:1443–1451.
11. Carey, M.A., et al. 2007. It's all about sex: gender, lung development and lung disease. *Trends Endocrinol. Metab.* **18**:308–313.
12. McCarthy, V.A., and Harris, A. 2005. The CFTR gene and regulation of its expression. *Pediatr. Pulmonol.* **40**:1–8.
13. Demko, C.A., Byard, P.J., and Davis, P.B. 1995. Gender differences in cystic fibrosis: Pseudomonas aeruginosa infection. *J. Clin. Epidemiol.* **48**:1041–1049.
14. Block, J.K., et al. 2006. Predictors of pulmonary exacerbations in patients with cystic fibrosis infected with multi-resistant bacteria. *Thorax.* **61**:969–974.
15. Rosenfeld, M., Davis, R., FitzSimmons, S., Pepe, M., and Ramsey, B. 1997. Gender gap in cystic fibrosis mortality. *Am. J. Epidemiol.* **145**:794–803.
16. Kaza, V., Katz, M.F., Cumming, S., Frost, A.E., and Safdar, Z. 2007. Correlation of chest radiograph pattern with genotype, age, and gender in adult cystic fibrosis: a single-center study. *Chest.* **132**:569–574.
17. Hess, R.A. 2003. Estrogen in the adult male reproductive tract: a review. *Reprod. Biol. Endocrinol.* **1**:52.
18. Jensen, E.V., and DeSombre, E.R. 1973. Estrogen-receptor interaction. *Science.* **182**:126–134.
19. Morley, P., Whitfield, J.F., Vanderhyden, B.C., Tsang, B.K., and Schwartz, J.L. 1992. A new, nongenomic estrogen action: the rapid release of intracellular calcium. *Endocrinology.* **131**:1305–1312.
20. Haynes, M.P., Russell, K.S., and Bender, J.R. 2000. Molecular mechanisms of estrogen actions on the vasculature. *J. Nucl. Cardiol.* **7**:500–508.
21. Le Mellay, V., Lasmoles, F., and Lieberherr, M. 1999. Galpha(q/11) and gbetagamma proteins and membrane signaling of calcitriol and estradiol. *J. Cell Biochem.* **75**:138–146.
22. Takemura, H., and Putney, J.W., Jr. 1989. Capacitative calcium entry in parotid acinar cells. *Biochem. J.* **258**:409–412.
23. Parekh, A.B., and Putney, J.W., Jr. 2005. Store-operated calcium channels. *Physiol. Rev.* **85**:757–810.
24. Lazarowski, E.R., Watt, W.C., Stutts, M.J., Boucher, R.C., and Harden, T.K. 1995. Pharmacological selectivity of the cloned human P2U-purinoceptor: potent activation by diadenosine tetraphosphate. *Br. J. Pharmacol.* **116**:1619–1627.
25. Huang, P., et al. 2001. Compartmentalized autocrine signaling to cystic fibrosis transmembrane conductance regulator at the apical membrane of airway epithelial cells. *Proc. Natl. Acad. Sci. U. S. A.* **98**:14120–14125.
26. Sweezey, N.B., et al. 2007. Amiloride-insensitive nasal potential difference varies with the menstrual cycle in cystic fibrosis. *Pediatr. Pulmonol.* **42**:519–524.
27. Kerem, E., Reisman, J., Corey, M., Canny, G.J., and Levison, H. 1992. Prediction of mortality in patients with cystic fibrosis. *N. Engl. J. Med.* **326**:1187–1191.
28. Verma, N., Bush, A., and Buchdahl, R. 2005. Is there still a gender gap in cystic fibrosis? *Chest.* **128**:2824–2834.

29. Arrington-Sanders, R., et al. 2006. Gender differences in health-related quality of life of adolescents with cystic fibrosis. *Health Qual. Life Outcomes.* **4**:5.
30. Lesmeister, M.J., Jorgenson, R.L., Young, S.L., and Misfeldt, M.L. 2005. 17Beta-estradiol suppresses TLR3-induced cytokine and chemokine production in endometrial epithelial cells. *Reprod. Biol. Endocrinol.* **3**:74.
31. Mollerup, S., Jorgensen, K., Berge, G., and Haugen, A. 2002. Expression of estrogen receptors alpha and beta in human lung tissue and cell lines. *Lung Cancer.* **37**:153–159.
32. Thomas, L., Doyle, L.A., and Edelman, M.J. 2005. Lung cancer in women: emerging differences in epidemiology, biology, and therapy. *Chest.* **128**:370–381.
33. Bulayeva, N.N., Wozniak, A.L., Lash, L.L., and Watson, C.S. 2005. Mechanisms of membrane estrogen receptor-alpha-mediated rapid stimulation of Ca2+ levels and prolactin release in a pituitary cell line. *Am. J. Physiol. Endocrinol Metab* **288**:E388–E397.
34. Perret, S., Dockery, P., and Harvey, B.J. 2001. 17beta-oestradiol stimulates capacitative Ca2+ entry in human endometrial cells. *Mol. Cell. Endocrinol.* **176**:77–84.
35. Knight, G.E., and Burnstock, G. 2004. The effect of pregnancy and the oestrus cycle on purinergic and cholinergic responses of the rat urinary bladder. *Neuropharmacology.* **46**:1049–1056.
36. Chaban, V.V., and Micevych, P.E. 2005. Estrogen receptor-alpha mediates estradiol attenuation of ATP-induced Ca2+ signaling in mouse dorsal root ganglion neurons. *J. Neurosci. Res.* **81**:31–37.
37. Chaban, V.V., Mayer, E.A., Ennes, H.S., and Micevych, P.E. 2003. Estradiol inhibits atp-induced intracellular calcium concentration increase in dorsal root ganglia neurons. *Neuroscience.* **118**:941–948.
38. Korngreen, A., Ma, W., Priel, Z., and Silberberg, S.D. 1998. Extracellular ATP directly gates a cation-selective channel in rabbit airway ciliated epithelial cells. *J. Physiol.* **508**:703–720.
39. Zsembery, A., et al. 2003. Sustained calcium entry through P2X nucleotide receptor channels in human airway epithelial cells. *J. Biol. Chem.* **278**:13398–13408.
40. Sun, H., Tsunenari, T., Yau, K.W., and Nathans, J. 2002. The vitelliform macular dystrophy protein defines a new family of chloride channels. *Proc. Natl. Acad. Sci. U. S. A.* **99**:4008–4013.
41. Schwiebert, E.M., et al. 1995. CFTR regulates outwardly rectifying chloride channels through an autocrine mechanism involving ATP. *Cell.* **81**:1063–1073.
42. Caputo, A., et al. 2008. TMEM16A, a membrane protein associated with calcium-dependent chloride channel activity. *Science.* **322**:590–594. doi:10.1126/science.1163518.
43. Yang, Y.D., et al. 2008. TMEM16A confers receptor-activated calcium-dependent chloride conductance. *Nature.* **455**:1210–1215. doi:10.1038/nature07313.
44. Wang, E.E., Prober, C.G., Manson, B., Corey, M., and Levison, H. 1984. Association of respiratory viral infections with pulmonary deterioration in patients with cystic fibrosis. *N. Engl. J. Med.* **311**:1653–1658.
45. Katzenellenbogen, B.S., et al. 2000. Molecular mechanisms of estrogen action: selective ligands and receptor pharmacology. *J. Steroid Biochem. Mol. Biol.* **74**:279–285.
46. Southern, K.W., et al. 2001. A modified technique for measurement of nasal transepithelial potential difference in infants. *J. Pediatr.* **139**:353–358.
47. Tarran, R., et al. 2002. Regulation of murine airway surface liquid volume by CFTR and Ca^{2+}-activated Cl^- conductances. *J. Gen. Physiol.* **120**:407–418.
48. Jefferson, D.M., et al. 1990. Expression of normal and cystic fibrosis phenotypes by continuous airway epithelial cell lines. *Am. J. Physiol.* **259**:L496–L505.
49. Lazarowski, E.R., and Harden, T.K. 1999. Quantitation of extracellular UTP using a sensitive enzymatic assay. *Br. J. Pharmacol.* **127**:1272–1278.
50. Tarran, R., et al. 2001. The CF salt controversy: in vivo observations and therapeutic approaches. *Mol. Cell.* **8**:149–158.